Serotonergic Modulation

Grady Kestler
University of California, San Diego
gradykestler@gmail.com

Ed Kantz
University of California, San Diego
ekantz@eng.ucsd.edu

Bryce Ito
University of California, San Diego
btito@eng.ucsd.edu

Abstract

In this project, we implemented models for serotonin modulation in biological neural networks, motivated by the findings of reduced serotonin neurotransmission as a consequence of Diabetes Mellitus. Because the effects of serotonin on the human nervous system are widely varying and poorly quantified, we used models based on experimental data for the model organism *Aplysia*. These models were used to investigate modified neurotransmission of serotonin in a single sensory neuron and in small neural networks. We also examined the effect on excitability and network performance. Finally, we investigated its implications on memory in a simple two-neuron circuit by experimenting with Hebbian learning rules and synaptic strengths. Our simulations indicate that reduced serotonin neurotransmission reduces the excitability of single neurons and impairs the function of simple neural networks. Our simulations involving synaptic plasticity indicate that reduced serotonin neurotransmission reduced or negated synaptic strengthening based on the implemented learning rules. The results provide basis for further experimental investigation to quantify the effect of serotonin in its varied roles in the human nervous system.

1 Introduction

1.1 Motivation

Diabetes is a group of metabolic diseases that a 2010 study found afflicts about 289 million adults worldwide, with an even greater prevalence in North America[6]. It has two main forms. Type 1 diabetes, or juvenile diabetes, is the result of an autoimmune disease that causes the body to be unable to produce sufficient insulin. Type 2 diabetes is the more common form and typically occurs in adults. This form is characterized by the body forming a resistance to the effects of insulin[5]. However, both forms are similar in that they lead to a decreased ability of the body to regulate its blood glucose levels. This leads to an increased occurrence of both hypoglycemia and hyperglycemia. Both can cause neurological complications. Extreme episodes can even result in permanent brain function impairment[4].

1.2 Background

Diabetes is known to cause changes in the levels of three main neurotransmitters: dopamine, norepinephrine, and serotonin. Hyperglycemia has been shown to depress the levels of dopamine in the brain. Hypoglycemia has been shown to increase the norepinephrine content[4]. However, some of the most significant effects are seen in serotonin. Without treating the diabetes, serotonin synthesis and neurotransmission can be decreased. Hyperglycemic rats have shown a decrease of up to 70% in serotonin levels[7]. The lack of serotonin in the brain can have several consequences, including thermoregulatory issues, dramatic mood swings, and a decrease in reproductive hormone levels[3].

In order to help treat the effects of diabetes on the central nervous system, a better understanding of the underlying mechanisms is desired. To this end, *Aplysia* is used. This genus of sea slugs is widely used in neurophysiology as a model organism for modeling of neural networks due to its simple neuronal structure and easily identified tail and gill withdrawl reflex. In the past, these models have led to crucial discoveries for the treatment of diseases such as Rubinstein-Taybi syndrome and hyperaglesia[1]. We will be using an *Aplysia* model to simulate the effects of lowered serotonin on neural networks with the hope that the data can be applied to guide the development of treatments for the effects of diabetes on the central nervous system.

1.3 Model of Serotonergic Modulation of Sensory Neurons in *Aplysia*

1.3.1 Scope and Purpose of Model

Voltage-clamp studies of *Aplysia* sensory neurons involved in the gill and tail withdrawal reflexes have shown that serotonin induces spike broadening and increased excitability. Studies completed during the 1980s and 1990s helped delineate the multiple pathways through which serotonergic modulation occurs in these cells. The following diagram (Figure 1) illustrates these pathways.

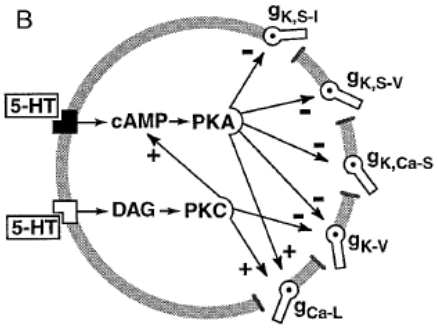

Figure 1: Pathways of Serotonergic Modulation
in *Aplysia* Neurons [2]

As shown in the figure, there are two separate pathways, associated with two distinct 5-hydroxytryptamine (5-HT) serotonin receptors, by which serotonergic modulation occurs. In one pathway, the binding of serotonin to the receptor releases cyclic adenosine monophosphate (cAMP) which acts as a second messenger activating protein kinase A (PKA). In the other pathway, diacyglycerol (DAG) acts as a second messenger, activating protein kinase C (PKC). PKA and PKC, in turn, modulate the membrane soma conductances as shown.

Baxter et al. sought to develop a model that would successfully replicate the empirical data obtained from the studies that identified the pathways, and could also be used to predict the spiking behavior of these neurons

in such a way that the model could be experimentally validated by in-vitro testing [2]. The group was able to accomplish this task by developing a Hodgkin-Huxley type model using the program SNNAP (Simulator for Neural Networks and Action Potentials).

Once the model was validated, it was used to determine what role the individual pathways had in causing the observed spike broadening and increased excitability.

1.3.2 Details of Modified HH Dynamics

The model developed by Baxter et al.[2] is a modified Hodgkin-Huxley model. The membrane voltage equation is expressed by

$$-C\frac{dV_m}{dt} = \left(\sum_{ion} I_{ion}\right) - I_{stim}$$

$$I_{ion} = g_{ion}(V_m - E_{ion}) \tag{1}$$

Where g_{ion} and E_{ion} represent the conductance and reversal potential of each ion respectively. The term g_{ion} was found using

$$g_{ion} = g_{max(ion)} A_{ion}^{p}(V_m, t) B_{ion}(V_m, t) \tag{2}$$

$A(V_m, t)$ and $B(V_m, t)$ are the voltage and time dependent activation and deactivation functions associated with each ion conductance defined by the following differential equations.

$$\frac{dA_{ion}}{dt} = \frac{A_{\infty(ion)} - A_{ion}}{\tau_{A(ion)}}$$

$$\frac{dB_{ion}}{dt} = \frac{B_{\infty(ion)} - B_{ion}}{\tau_{B(ion)}}$$

$$A_{\infty(ion)} = \frac{1}{1 + exp((V_m - h_{A(ion)})/s_{A(ion))}}$$

$$B_{\infty(ion)} = \frac{1 - B_{min(ion)}}{(1 + exp((V_m - h_{B(ion)})/s_{B(ion)}))^{p_B}} + B_{min(ion)}$$

$$\tau_{A(ion)} = \frac{\tau_{A(max)(ion)} - \tau_{A(min)(ion)}}{(1 + exp((V_m - h_{\tau A(ion)})/s_{\tau A(ion)}))^{n_A}} + \tau_{A(min)(ion)}$$

$$\tau_{B(ion)} = \frac{\tau_{B(max)(ion)} - \tau_{B(min)(ion)}}{(1 + exp((V_m - h_{\tau B(ion)})/s_{\tau B(ion)}))^{n_B}} + \tau_{B(min)(ion)} \tag{3}$$

g_{max}, maximum conductance; h_A, half-activation voltage; s_A, slope parameter of activation function; p, power of activation function; $A_{(max)}$, maximal value of activation time constant; $A_{(min)}$, minimum activation time constant; $h_{\tau A}$, voltage at which activation time constant is half-maximal; $s_{\tau A}$, slope parameter of activation time constant function; h_b, half-inactivation voltage; s_B, slope parameter of inactivation function; $B_{(max)}$, maximum value of inactivation time constant; $B_{(min)}$, minimum value of inactivation time constant; $h_{\tau B}$, voltage at which inactivation time constant is half-maximal; $s_{\tau B}$, slope parameter of inactivation time constant function. [2]

The value p_B was 1.0 for all ions except for the the voltage dependent potassium current, I_{K-V}, for which it was 2.0. The value n_A were 2.0 for the currents, $I_{Ca-L}, I_{Ca-N}, I_{K-A}$, and $I_{K,S-V}$, and 1.0 for all others. Likewise, the value n_B were 2.0 for the currents, I_{Ca-L}, I_{Ca-N}, and I_{K-V}, and 1.0 for all others.

In addition to this modified Hodgkin Huxley model, Baxter et al included modulation of currents due to intracellular calcium concentrations. We included these as part of the SNNAP simulations and experiments, but excluded them from the Python simulations and experiments. These additional details are included in Appendix B.

2 Methods

2.1 SNNAP Model of Single Neuron

The model developed by Baxter et al. was created using the program SNNAP. This program was developed by Ziv et al. [10] at the University of Texas Medical School at Houston, in the early 1990s. The program was created to simulate single neurons and small neural networks using built-in mathematical descriptions of neuron dynamics. The current version of the program is written in JAVA and includes a graphical user interface. [8]

In order to reduce the likelihood of introducing errors into our reproduction of the model developed by Baxter et al., we also utilized SNNAP for a number of our models and simulations.

First, the model developed by Baxter et al. was recreated from the partial model acquired from the SNNAP website [8]. The partial model included the mathematical descriptions of the various single neuron scenarios developed by Baxter et al. and only simulation files and output files needed to be created to check that the simulator was producing the same results obtained by Baxter et al.

After obtaining the expected identical simulation results, the model was then altered to investigate the effect of reducing the serotonergic modulation in a way that may be comparable to reduction in serotonin neurotransmission observed in the brains of diabetic rats. This was accomplished by altering the parameters describing the serotonergic modulation membrane currents. These parameters (ion channel conductances and time constants) are shown in Table 1.

Serotonin transmission in diabetic rat brains was shown to be reduced by 40-70% [7]. For clarity of illustration, values were selected for the parameters that were halfway between the values for the control (no serotonergic modulation) and the normal serotonergic modulation provided by Baxter et al. These values should approximately correspond to serotonergic transmission reduction of 50% and are shown in Table 1.

2.2 Application to Simple Neural Network

In addition to examining the effects of reduced serotonin on the single neuron, we also expanded our analysis to include a simple neural network. The neural network we utilized was based on a three layer network

Current/Parameter	Control	Full 5-HT-Induced Modulation	50% 5-HT-Induced Modulation
$I_{K,S-V}$			
$g_{max}(mS)$	0.54	0.25	0.395
$I_{K,S-I}$			
$g_{max}(mS)$	0.012	0.006	0.009
$I_{K,S-I}$			
$g_{max}(mS)$	4.5	2.3	3.4
$\tau_{A(max)}(ms)$	32.5	55.5	44
$\tau_{A(min)}(ms)$	0.5	1.0	0.75
$\tau_{B(max)}(ms)$	1600.0	8200.0	4900
$\tau_{B(min)}(ms)$	5.0	50.0	27.5
I_{Ca-L}			
$g_{max}(mS)$	0.08	0.2	0.14
$I_{K,Ca-S}$			
$g_{max}(mS)$	0.158	0.036	0.097
$I_{Stim(bias)}$	0.0	-0.11	-0.055

Table 1: Modulated parameters.

developed by White et al. [9]. The model was originally developed to examine the role of interneurons in the extended responses of pedal motor neurons to tail stimulation in *Aplysia*.

White et al. found that a network consisting of only sensory neurons with excitatory synaptic connections to a motor neuron would not induce the long duration spiking in the motor neuron that had been observed in-vitro. However, when an additional layer of neurons modeled on the LP117 excitatory interneurons found in *Aplysia* was added to the network, the extended response could be reproduced. The architecture of the two neural networks and their responses to a test stimulating current are shown in Figure 2 and Figure 3.

In these networks, the four sensory neurons correspond to the neurons that would be stimulated by the standard tail pinch that is used to activate a tail withdrawal reflex in *Aplysia*, and the stimulating current pulse applied to the neurons represent the pinch itself.

The three-layer network used by White et al. is well suited for our purposes for several reasons. The network is based on the same model organism and the same tail withdrawal response that the Baxter et al. single sensory neuron model was based on. This allows us to be biologically consistent in our simulations. Additionally, the presence or absence of a delayed long duration spike chain in the motor neuron provides a clear and simple benchmark upon which to judge success or failure of the system.

The effect of reduced serotonergic modulation was tested using this neural network by replacing the four sensory neurons in the original network model with the sensory neurons developed for the single neuron simulations previously described, creating three distinct network cases each with 4 identical sensory neurons with either no serotonergic modulation, normal full serotonergic modulation, or 50% of the normal serotonergic modulation. Each of these three networks were then tested with stimulating current pulses of various magnitudes to determine if the long duration spike chain in the motor neuron would be triggered.

These simulations were performed with models developed using SNNAP and results of these simulations are shown in Figures 6 through 12.

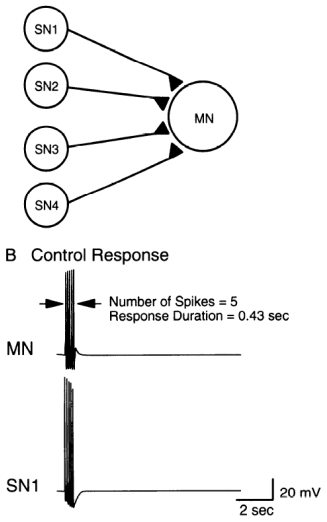

Figure 2: Two-layer network model developed by White et al. and associated spiking response [9]

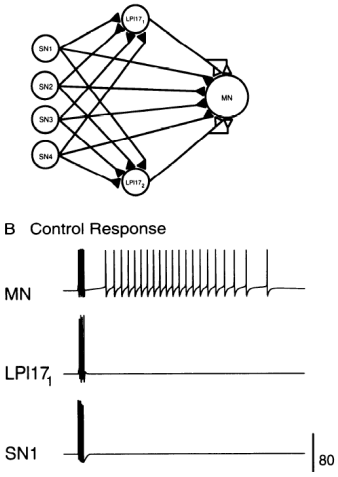

Figure 3: Three-layer network model developed by White et al. and associated spiking response [9]

2.3 Model Comparison

Not shown in Equations 1, 2, and 3, Baxter et al included a calcium induced modulation of the currents, I_{K-Ca}, I_{Ca-L}, and I_{Ca-N}. We did not account for this extra modulation in our Python Hebbian learning models, but properly adjusted the given parameters to match each of the current simulations from Baxter et al. Each of the simulated currents from our implementation and the simulations from Baxter et al are found in Appendix A.

For the I_{Ca-N} current, we adjusted $h_{\tau A}$ from 3.0 to 0.0. This value represents the voltage at which the time constant of the activation is half-maximal meaning that lowering it would cause the current to activate more quickly for higher voltages. For the I_{K-Ca} current, we adjusted the $\tau_{A(max)}$ and $\tau_{A(min)}$ to 200.0 and 100.0 from 0.0 respectively. These values represent the maximum value of the activation time constant and the minimum value of the activation time constant. By increasing them from 0.0, we forced the I_{K-Ca} current to not be instantaneous. Besides these adjustments, the same values were used that can be found in Baxter et al [2].

3 Results

3.1 Results of Single Neuron Simulations

The two stimulating current scenarios used by Baxter et al. in their single-neuron model were repeated with the original inputs for no serotonin and normal serotonin, as well as the values representing 50% reduction. The simulation results are shown in Figure 4 and Figure 5.

The spike broadening effect of serotonin observed in the *Aplysia* sensory neurons and simulated by Baxter et al. is reproduced in Figure 4. This figure also includes the simulated results of the neuron with a 50% sero-

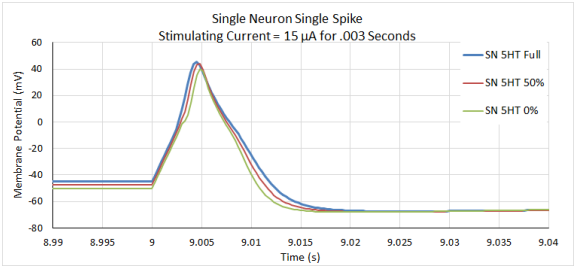

Figure 4: Spike broadening resulting from serotonin modulation

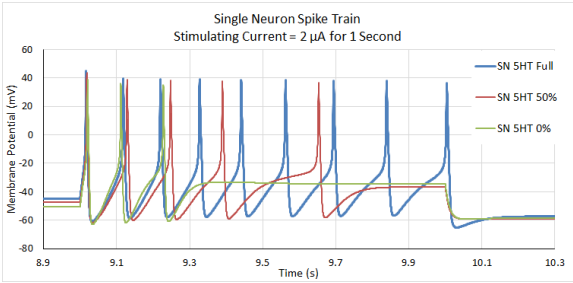

Figure 5: Increased excitability resulting from serotonin modulation

tonin modulation stimulated by the same current. The result indicates that the reduced serotonin produced a spike broadening effect relative to the control (no serotonin) but less than the normal serotonin case.

Similarly, Figure 5 shows that a longer current pulse ($2\mu A$ for 1 second) elicits continued spiking only in the neuron with normal full serotonergic modulation while the control case only spikes three times and the 50% serotonergic case spikes an intermediate value of 5 times.

3.2 Results of Network Simulations

The results of the small network simulations with stimulating current pulse of $5\mu A$ applied for 0.4 seconds are shown in Figures 6, 7, and 8. Note that Figure 6 shows the spiking output of one of the sensory neurons, where spiking occurs only during the duration of the stimulating current pulse. Figure 7 shows the spiking of the motor neuron during the current pulse and Figure 8 shows the spiking of the motor neuron that occurs after the stimulating current pulse has completed as can be noted from the time scale on the x-axis. With this stimulating current, all three neuron types produced the delayed long duration spiking in the motor neuron.

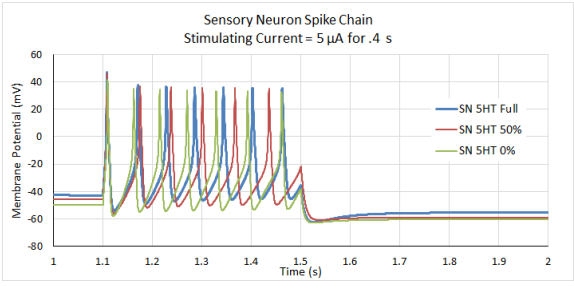

Figure 6: Sensory neuron spiking from $5\mu A$ stimulating pulse

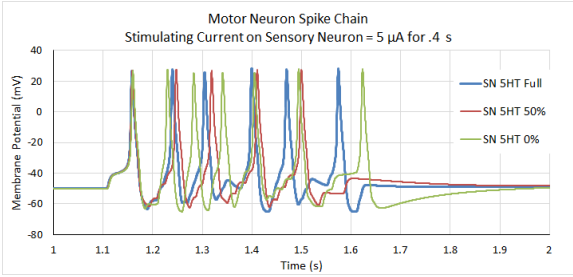

Figure 7: Motor neuron spiking during $5\mu A$ pulse

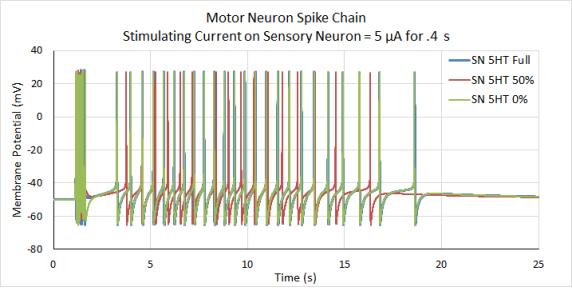

Figure 8: Extended motor neuron spiking resulting from $5\mu A$ pulse

The stimulating current was reduced in two additional simulations. The results of these simulations are shown in Figures 9 through 12. When the stimulating current was reduced to $2\mu A$ (Figure 9 and Figure 10) the unmodulated sensory neurons failed to produce the extended spiking in the motor neuron and at $1.5\mu A$ (Figure 11 and Figure 12) only the sensory neurons with the full serotonergic modulation produced that effect.

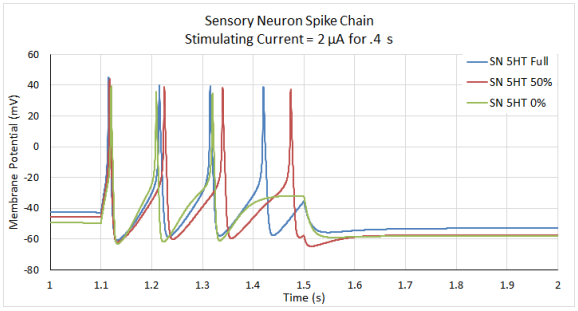

Figure 9: Sensory neuron spiking from stimulating current of $2\mu A$ for 0.4 seconds

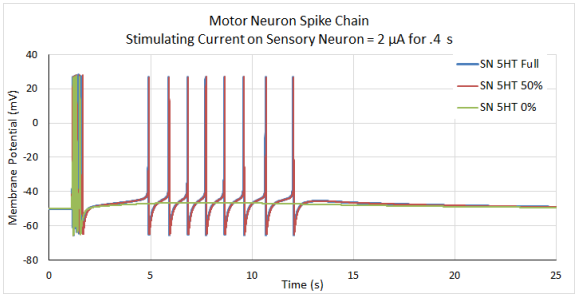

Figure 10: Motor neuron spiking resulting from stimulating current of $2\mu A$ for 0.4 seconds

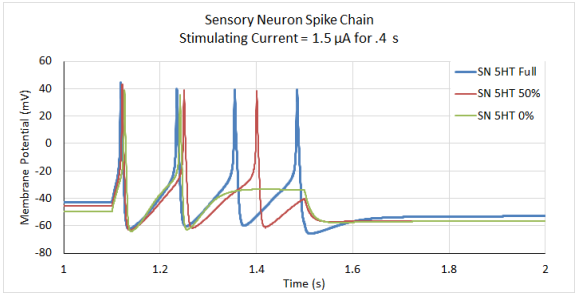

Figure 11: Sensory neuron spiking from stimulating current of $1.5\mu A$ for 0.4 seconds

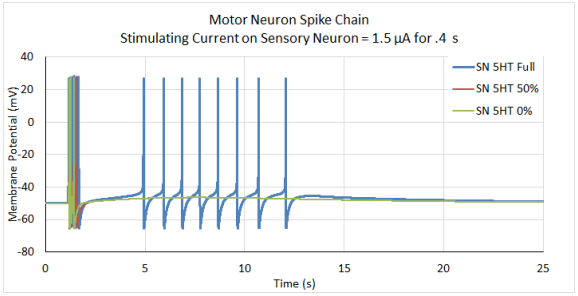

Figure 12: Motor neuron spiking resulting from stimulating current of $1.5\mu A$ for 0.4 seconds

3.3 Python Implementation and Hebbian Learning

Using the proper control values from Table 1 and Appendix B, an injection current of $7\mu A$ was applied to a single neuron for two seconds in order to observe a single spike. Figure 13 illustrates this effect. With 100% serotonin modulation of the neuron, we applied the same current, $7\mu A$ over the same time scale, two seconds, and observed a much higher frequency of spiking as shown in Figure 14. At 50% and 75% serotonin modulation, we observed a spiking frequency in between both the control and the 100% modulation. (Figures 15 and 16).

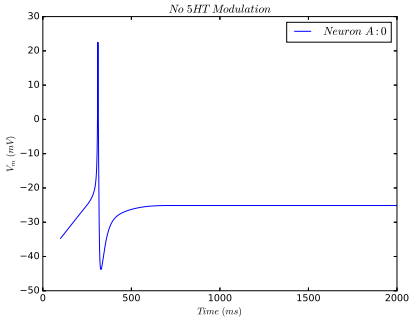

Figure 13: Single spike of a neuron injected with $7\mu A$ current for 2 seconds.

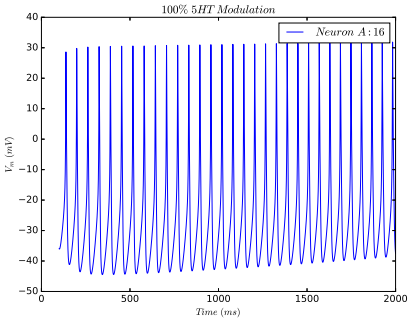

Figure 14: Spike train of a 100% serotonin modulated neuron injected with $7\mu A$ current for 2 seconds.

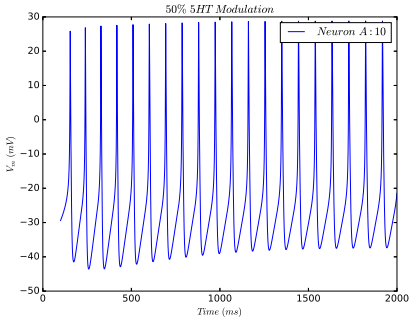

Figure 15: Spike of a 50% serotonin modulated neuron injected with $7\mu A$ current for 2 seconds.

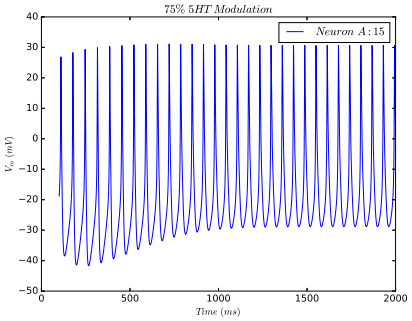

Figure 16: Spike train of a 75% serotonin modulated neuron injected with $7\mu A$ current for 2 seconds.

We then expanded the model to account for a single excitatory synapse connection between two neurons, A and B, both affected by serotonin modulation. We used a simple glutamate conductance to adjust the connection strength between the two neurons. Equation 1 became

$$-C\frac{dV_m}{dt} = \left(\sum_{ion} I_{ion} + I_{esyn}\right) - I_{stim}$$

where

$$I_{esyn} = g_{Glu} r(V_m - E) \qquad\qquad E = -10.0$$

and

$$\frac{dr}{dt} = 2.8 T_e(V_m)(1 - r) - (.3r)$$

$$T_e(V_m) = \frac{1}{1 + exp(-(V_m - 10.0)/15.0)}$$

Because of the increase in firing rate between the different modulations of serotonin, we implemented a Hebbian learning rule which modified the glutamate conductance of the synapse as a function of spike frequency of neuron A.

$$g_{Glu} = \frac{1}{(1 + exp(-(freq - 10.0)/3.0)}$$

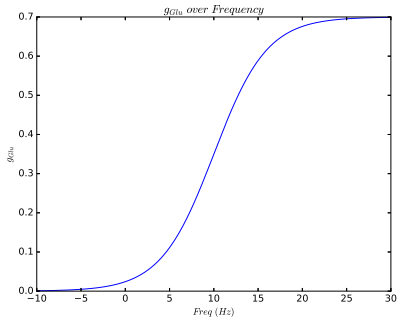

Figure 17: Hebbian learning rule for changing conductance as a function of spiking frequency of neuron A.

As the frequency of the spiking rate increased, the glutamate conductance increased and approached 0.7. If the frequency of the spiking rate decreased towards 0 Hz, the glutamate conductance decreased to 0 indicating a weak connection between the neurons. Figures 18, 19 20, and 21, illustrate the firing of both neurons. It can be observed between the two firing rates that increasing the serotonin modulation does increase the firing rate of the second neuron while decreasing the serotonin modulation has a reverse affect. One improvement that should be made is for the synaptic strength to continually change based on the frequency. In Figure 20, we observe that the strength remains static since the frequency is static. Only with 100% and 75% modulation does the synapse continue to strengthen.

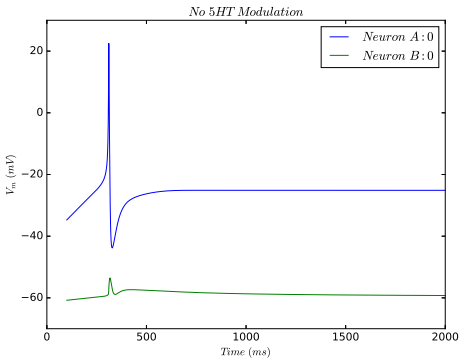

Figure 18: Single spike of a neuron injected with $7\mu A$ current for 2 seconds.

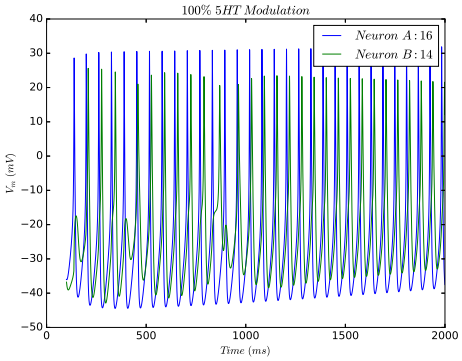

Figure 19: Spike train of a 100% serotonin modulated neuron injected with $7\mu A$ current for 2 seconds.

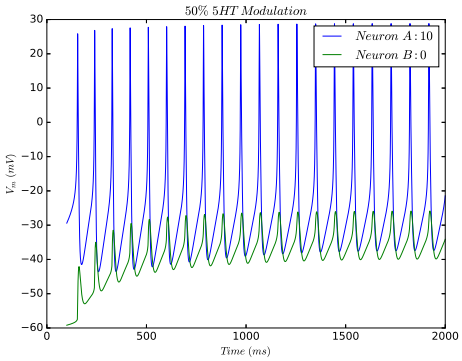

Figure 20: Spike of a 50% serotonin modulated neuron injected with $7\mu A$ current for 2 seconds.

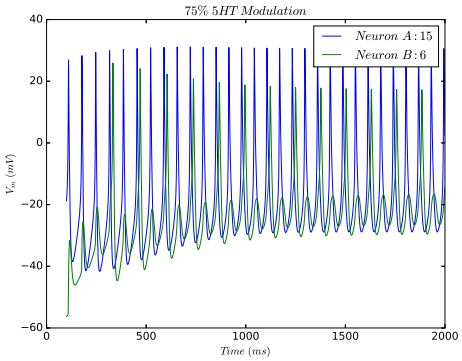

Figure 21: Spike train of a 75% serotonin modulated neuron injected with $7\mu A$ current for 2 seconds.

4 Conclusions

4.1 Conclusions from the Single Neuron and Simple Network Models

Adding an intermediate serotonergic modulation scenario to the Baxter et al. single sensory neuron model further illustrated the role of serotonin in this model. The results of the simple neural network simulations of the three different sensory neurons illustrate the importance of serotonergic modulation in a network setting. Even though the interneurons and the motor neurons in the simple network did not have serotonin 5HT receptors, the reduction in serotonin neurotransmission in the sensory neurons significantly altered their spiking output and the function of the network as a whole. In the modeled network, the altered output of the motor neuron in the cases where the sensory neurons did not receive the normal level of serotonergic modulation may manifest as a lack of tail withdrawal of the organism in response to a stimulus that would normally elicit that reflex.

4.2 Implications to Learning

Consistent with Baxter et al. [2], we found that the serotonin modulation increased the firing rate of neurons with 5HT receptors. Hebbian learning rules indicate that neurons spiking in a correlated fashion, increase the synaptic strength between them. By implementing a crude Hebbian model of glutamate conductance of the synapse, we were able to perceive that serotonergic modulation does affect synapse strengths. In order to classify this increase, we plotted the normalized cross-correlation between the two neurons in Figure 22. Our spiking threshold was set at 10.0 mV implying that any voltage change less than 10.0 mV is not considered a spike and should not be included in the correlation calculation. The 0% and 50% modulation elicited no spiking of neuron B and therefor there is no correlation between the two neurons in these trials. Looking at the 75% and 100% modulated firings, we see a stronger correlation over time in both, however, the 100% modulated neurons indicate a slightly higher correlation. This corresponds to a slightly stronger synapse.

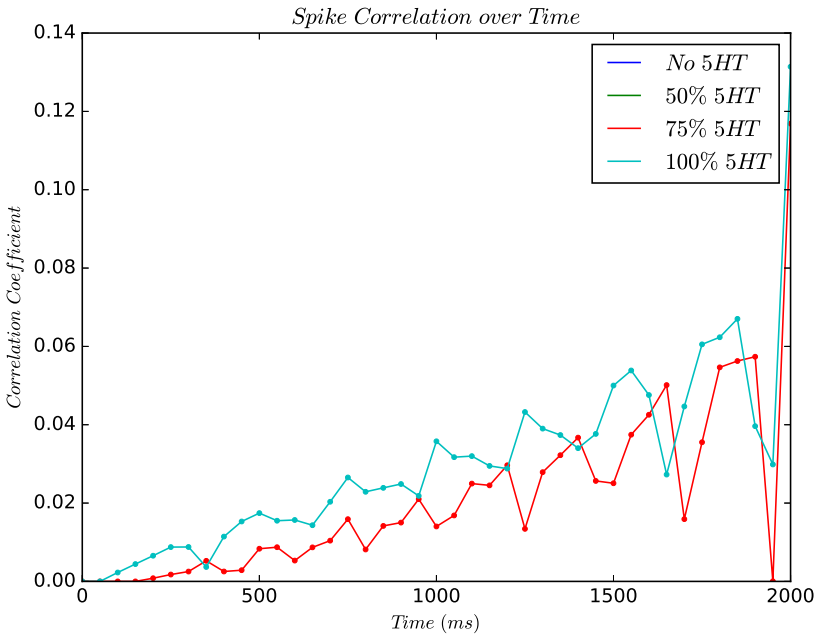

Figure 22: Spike correlation of 100% and 75% serotonin modulated neurons.

4.3 Future Directions

This work could be expanded in several different directions. The Hebbian learning model could be edited to make it more robust. In its current state, there are several assumptions and simplifications made that could be improved, adding both accuracy and complexity to the model. The model could be improved by including spike-timing-dependent plasticity (STDP) as a more detailed model than the Hebbian model that was used. Also, the levels of 5-HT modulation in the neurons could be adjusted to more closely approximate observed effects.

Although we created a working model of serotonergic modulation, it was based on data gathered from *Aplysia*. Ample data are available on *Aplysia* due to its simple nervous system which is easy to study. In order

to have specific clinical value, this type of model would need to be based on human data. The human nervous system is much more complex and cannot be studied in the same way as model organisms like *Aplysia*, so presently data providing specific quantification of serotonin's effects on human neurons is not available. The research that has been completed indicates that serotonin plays many different roles in the human nervous system, so any model developed indicating the effects of reduced serotonin neurotransmission in humans would need to be very specific in the part of the nervous system being modeled, or very complex to accurately simulate serotonin's multiple roles. Present treatments for serotonin neurotransmission disorders, such as selective serotonin reuptake inhibitors (SSRIs), have effects on the full nervous system and some of these effects are negative and unintended. For this reason, the development of more detailed models of the effects of altered serotonin transmission in humans is warranted to help guide the development of more targeted treatments.

References

[1] Thomas W. Abrams. Studies on Aplysia neurons suggest treatments for chronic human disorders. *Current Biology*, 22(17):R705–R711, 2012.

[2] Douglas A Baxter, Carmen C Canavier, John W Clark, and John H Byrne. Computational Model of the Serotonergic Modulation of Sensory Neurons in Aplysia.

[3] T.S. King and D.H. Rohrbach. Reduced aminergic synthesis in the hypothalamus of the infertile, genetically diabetic (C57BL/KsJ-db/db) male mouse. *Exp Brain Res*, 81:619–625, 1990.

[4] Anthony L. McCall. Perspectives in Diabetes The Impact of Diabetes on the CNS. *Diabetes*, 41(May):557–70, 1992.

[5] Dominique L. Musselman, Ephi Betan, Hannah Larsen, and Lawrence S. Phillips. Relationship of depression to diabetes types 1 and 2: Epidemiology, biology, and treatment. *Biological Psychiatry*, 54(3):317–329, 2003.

[6] J. E. Shaw, R. A. Sicree, and P. Z. Zimmet. Global estimates of the prevalence of diabetes for 2010 and 2030. *Diabetes Research and Clinical Practice*, 87(1):4–14, 2010.

[7] Michael E Trulson, Jacob H Jacoby, and Robert G Mackenzie. Streptozotocin-Induced Diabetes Reduces Brain Serotonin Synthesis in Rats. 1986.

[8] University of Texas Houston. Department of Neurobiology and Anatomy — SNNAP - UTHealth Medical School, 2008.

[9] J a White, I Ziv, L J Cleary, D a Baxter, and J H Byrne. The role of interneurons in controlling the tail-withdrawal reflex in Aplysia: a network model. *Journal of neurophysiology*, 70(5):1777–1786, 1993.

[10] Israel Ziv, D a Baxter, and J H Byrne. Simulator for neural networks and action potentials: description and application. *Journal of neurophysiology*, 71(1):294–308, 1994.

Appendix A Simulation Results Comparison

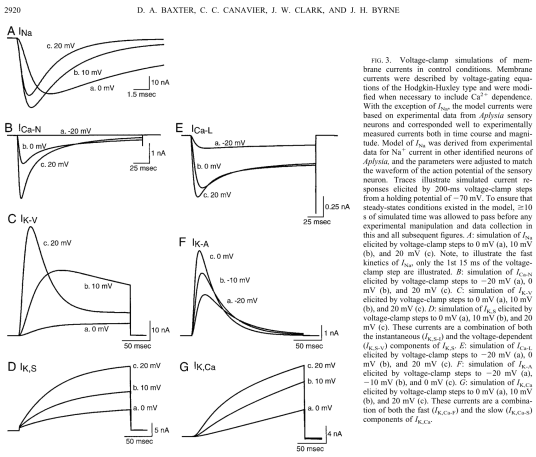

FIG. 3. Voltage-clamp simulations of membrane currents in control conditions. Membrane currents were described by voltage-gating equations of the Hodgkin-Huxley type and were modified when necessary to include Ca^{2+} dependence. With the exception of I_{Na}, the model currents were based on experimental data from *Aplysia* sensory neurons and corresponded well to experimentally measured currents both in time course and magnitude. Model of I_{Na} was derived from experimental data for Na^+ current in other identified neurons of *Aplysia*, and the parameters were adjusted to match the waveform of the action potential of the sensory neuron. Traces illustrate simulated current responses elicited by 200-ms voltage-clamp steps from a holding potential of −70 mV. To ensure that steady-states conditions existed in the model, ≥10 s of simulated time was allowed to pass before any experimental manipulation and data collection in this and all subsequent figures. *A*: simulation of I_{Na} elicited by voltage-clamp steps to 0 mV (a), 10 mV (b), and 20 mV (c). Note, to illustrate the fast kinetics of I_{Na}, only the 1st 15 ms of the voltage-clamp step are illustrated. *B*: simulation of I_{Ca-N} elicited by voltage-clamp steps to −20 mV (a), 0 mV (b), and 20 mV (c). *C*: simulation of I_{K-V} elicited by voltage-clamp steps to 0 mV (a), 10 mV (b), and 20 mV (c). *D*: simulation of $I_{K,S}$ elicited by voltage-clamp steps to 0 mV (a), 10 mV (b), and 20 mV (c). These currents are a combination of both the instantaneous ($I_{K,S,f}$) and the voltage-dependent ($I_{K,S,V}$) components of $I_{K,S}$. *E*: simulation of I_{Ca-L} elicited by voltage-clamp steps to −20 mV (a), 0 mV (b), and 20 mV (c). *F*: simulation of I_{K-A} elicited by voltage-clamp steps to −20 mV (a), −10 mV (b), and 0 mV (c). *G*: simulation of $I_{K,Ca}$ elicited by voltage-clamp steps to 0 mV (a), 10 mV (b), and 20 mV (c). These currents are a combination of both the fast ($I_{K,Ca,f}$) and the slow ($I_{K,Ca,s}$) components of $I_{K,Ca}$.

Figure 23: Simulations performed by Baxter et al [2]

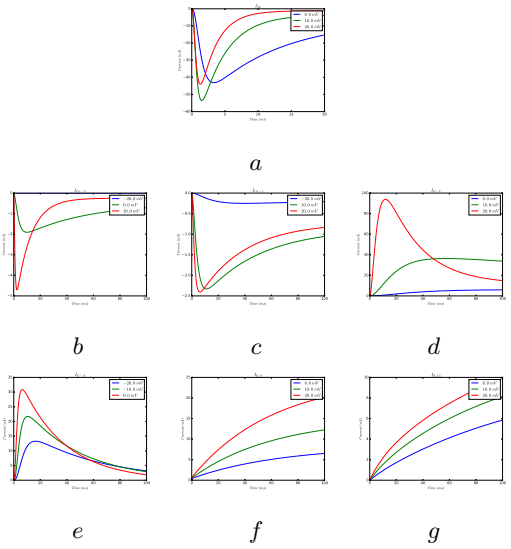

a

b *c* *d*

e *f* *g*

Figure 24: Simulations of model currents. (a) I_{Na} at 0.0, 10.0, and 20.0 mV. (b) I_{Ca-N} at -20.0, 0.0, and 20.0 mV. (c) I_{Ca-L} at -20.0, 0.0, and 20.0 mV. (d) I_{K-V} at 0.0, 10.0, and 20.0 mV. (e) I_{K-A} at -20.0, 0.0, and 20.0 mV. (f) I_{K-S} at 0.0, 10.0, and 20.0 mV. (g) I_{K-Ca} at 0.0, 10.0, and 20.0 mV.

Appendix B Additional Parameters and Equations Utilized from Baxter et al. Model

The full details of the Baxter et al. [2] model are provided in the original paper cited in the References section of this report.

The parameters from Table 1 of Baxter et al. [2] were used in the models.

TABLE 1. *Parameters describing membrane currents in control conditions*

Current	E_r, mV	g_{max}, μS	h_A, mV	s_A, mV	p	$\tau_{A(max)}$, ms	$\tau_{A(min)}$, ms	$h_{\tau A}$, mV	$s_{\tau A}$, mV	h_B, mV	s_B, mV	$\tau_{B(max)}$, ms	$\tau_{B(min)}$, ms	$h_{\tau B}$, mV	$s_{\tau B}$, mV
I_{Na}	60.0	2.5	−10.1	−9.8	3	1.5	0.45	−0.7	1.85	−19.5	9.2	15.0	2.4	2.8	3.5
$I_{Ca\text{-}N}$	60.0	0.16	0.15	−5.0	2	10.0	0.05	3.0 −4.0*	18.4 −4.6*	−15.0	11.0	620.0	3.72	−18.0 −20.0*	18.0 −15.0*
$I_{Ca\text{-}L}$	60.0	0.08	−7.4	−10.0	2	17.5	0.14	2.2 −15.0*	18.5 −12.0*	−33.0	49.5	20500.0	20.5	−125.0 −70.0*	40.0 −115.0*
$I_{K\text{-}A}$	−70.0	0.65	−45.0	−15.0	3	17.0	0.34	−20.0 −110.0*	20.0 −24.0*	−70.0	5.0	224.0	0.1	−54.4	30.8
$I_{K\text{-}V}$	−70.0	4.5	15.3	−8.4	2	32.5	0.5	15.0	8.2	7.9	1.5	1600.0	5.0	5.8 6.3*	3.3 −1.5*
$I_{K,S\text{-}V}$	−70.0	0.54	20.0	−15.0	1	255.0	61.2	−15.0 −46.0*	10.0 −6.5*						†
$I_{K,Ca\text{-}F}$	−65.0	0.02	23.5	−10.5	1	1.0‡									†
$I_{K,Ca\text{-}S}$	−65.0	0.158													§
$I_{K,S\text{-}I}$	−70.0	0.012	91.2	−84.8	1										§ §
I_L	−40.0	0.018													

The SNNAP model from Baxter et al. [2] accounted for intracelluar calcium modulation of certain currents. These modulations were accounted for using the following modified equations.

$$g_{ion} = g_{max(ion)} A_{ion}^{p}(V_m, t) B_{ion}(V_m, t)$$

$$\frac{d[Ca^{2+}]}{dt} = \frac{K_{Ca}(-\sum I_{Ca}) - [Ca^{2+}]}{\tau_{Ca}}$$

$$f[REG] = \begin{cases} gbr & \text{for enhancement} \\ \frac{1}{1+\beta.gbr} & \text{for attenuation} \end{cases}$$

$$\frac{d(gbr)}{dt} = \frac{[Ca^{2+}] - gbr}{\tau_{gbr}}$$

$$gbr = \frac{[Ca^{2+}]}{K_{Ca-(n)} + [Ca^{2+}]}$$

$\tau_{gbr} = 0.01s$ for $I_{K,Ca-F}$ and $\tau_{gbr} = 3s$ for $I_{K,Ca-S}$. Also, $I_{Ca-N} = 60$ and $K_{Ca-L} = 75$, and $\beta = 17$ for both I_{Ca-L} and I_{Ca-N}